Enhanced Protein Thermostability by Ala → Aib Replacement†

Vincenzo De Filippis, Filippo De Antoni, Marta Frigo, Patrizia Polverino de Laureto, and Angelo Fontana*

CRIBI Biotechnology Centre, University of Padua, via Trieste 75, 35121 Padua, Italy

Received August 6, 1997; Revised Manuscript Received November 3, 1997

ABSTRACT: The introduction into peptide chains of α-aminoisobutyric acid (Aib) has proven to stabilize the helical structure in short peptides by restricting the available range of polypeptide backbone conformations. In order to evaluate the potential stabilizing effect of Aib at the protein level, we have studied the conformational and stability properties of Aib-containing analogs of the carboxy-terminal subdomain 255−316 of thermolysin. Previous NMR studies have shown that this disulfide-free 62-residue fragment forms a dimer in solution and that the global 3D structure of each monomer (3 α-helices encompassing residues 260−274, 281−295, and 301−311) is largely coincident with that of the corresponding region in the X-ray structure of intact thermolysin. The Aib analogs of fragment 255−316 were prepared by a semisynthetic approach in which the natural fragment 255−316 was coupled to synthetic analogs of peptide 303−316 using V8-protease in 50% (v/v) aqueous glycerol [De Filippis, V., and Fontana, A. (1990) *Int. J. Pept. Protein Res. 35*, 219−227]. The Ala residue in position 304, 309, or 312 of fragment 255−316 was replaced by Aib, leading to the singly substituted fragments Ala304Aib, Ala309Aib, and Ala312Aib. Moreover, fragment Ala304Aib/Ala309Aib with a double Ala → Aib exchange in positions 304 and 309 was produced. Far- and near-UV circular dichroism measurements demonstrated that both secondary and tertiary structures of the natural fragment 255−316 are fully retained upon Ala → Aib substitution(s). Thermal unfolding measurements, carried out by recording the ellipticity at 222 nm upon heating, showed that the melting temperatures (T_m) of analogs Ala304Aib and Ala309Aib were 2.2 and 5.4 °C higher than that of the Ala-containing natural species (T_m = 63.5 °C), respectively, whereas the T_m of the Ala312Aib analog was lowered by −0.6 °C. The enhanced stability of the Ala304Aib analog can be quantitatively explained on the basis of a reduced backbone entropy of unfolding due to the restriction of the conformational space allowed to Aib in respect to Ala, while the larger stabilization observed for the Ala309Aib analog can be accounted for by both entropic and hydrophobic effects. In fact, whereas Ala304 is a surface residue, Ala309 is shielded from the solvent, and thus the enhanced stability of fragment Ala309Aib is also due to the burial of an additional -CH_3 group with respect to the natural fragment. The slightly destabilizing effect of the Ala → Aib exchange in position 312 appears to derive from unfavorable strain energy effects, since ϕ and ψ values for Ala312 are out of the allowed angles for Aib. Of interest, the simultaneous incorporation of Aib at positions 304 and 309 leads to a significant and additive increase of +8 °C in T_m. The results of this study indicate that the rational incorporation of Aib into a polypeptide chain can be a general procedure to significantly stabilize proteins.

Site-directed mutagenesis is an extremely valuable technique to replace amino acid residues at any desired position along the protein chains and thus to produce protein mutants for probing the effects of amino acid structure on protein function, folding, and stability (*1*, *2*). However, the method is restricted to the 20 genetically coded amino acids, whereas it is anticipated that the incorporation of noncoded amino acids with tailored side chains or even novel backbones into proteins would much expand the scopes of protein engineering, allowing more detailed and quantitative analysis of the effects of a given mutation on a specific protein property (*3*−*6*). Several approaches and techniques have been investigated in recent years for producing proteins containing unusual amino acids. A biosynthetic procedure using auxotrophic bacterial strains has been successfully employed to produce protein mutants containing phenylalanine analogs, *m*-fluorotyrosine, selenomethionine, or 7-azatryptophan (*7*, *8*). Schultz and co-workers (*9*−*14*) developed a method to produce proteins with unusual amino acids by using modified tRNA that is acylated with the noncoded amino acid and has a recognition site complementary to a stop codon. However, this procedure suffers yet from several limitations, including elaborate protection and deprotection strategies, very small quantities of mutated protein that can be obtained, unpredictable yields of amino acid incorporation, and the impossibility of introducing multiple substitutions in the same protein (*4*, *15*, *16*). Another option to introduce a large variety of noncoded amino acids or even nonpeptidic moieties into a polypeptide chain, the total chemical synthesis of proteins, is largely restricted to relatively short peptides,

† This work was supported by the Italian National Council of Research (CNR). Part of this study was presented at Perspectives in Protein Engineering, Montpellier (France), March 2−6, 1996 (Commun. 91B).

* Author to whom correspondence should be addressed (Telephone: +39-49-827-6156; Fax: +39-49-827-6159; E-mail: fontana@civ.bio.unipd.it).

S0006-2960(97)01937-5 CCC: $15.00
Published on Web 01/23/1998

since it is difficult to isolate in pure form the products of peptide synthesis when the desired polypeptide is longer than ~50 amino acids (*17*). To overcome these limitations, an approach which would allow both the preparation of relatively large proteins and the exploitation of the versatility of chemical synthesis is protein semisynthesis, defined as the covalent restitching of two polypeptide fragments, one of which is prepared by chemical methods (*18*−*20*). The more general procedure utilized so far in protein semisynthesis is the protease-catalyzed synthesis of the two fragments (natural and synthetic) in aqueous organic solvent, which favors synthesis over hydrolysis of peptide bonds by the protease (*21*).

α-Aminoisobutyric acid (Aib, or α-methylalanine)[1] is a natural, non-protein amino acid which has been found in membrane-channel-forming peptides of microbial origin (*22*). A variety of experimental studies conducted on short peptides have shown that Aib exclusively forms and stabilizes helical backbone structures (*23*, *24*). In particular, Aib favors the formation of 3_{10}-helices in homooligomers of Aib (*25*, *26*), while it stabilizes the α-helical structure when a single Aib residue is incorporated into a synthetic peptide (*27*). Moreover, Aib has been reported to possess a slightly higher intrinsic helical propensity than Ala, which is the most helix-favoring among the 20 protein amino acids (*28*, *29*). In this respect, theoretical studies have indicated that the helix-stabilizing effect of Aib is caused by the geminal methyl groups which severely reduce the allowed conformational space and restrict the peptide backbone torsion angles (ϕ, ψ) to those characteristic of the helical configuration (*27*, *29*−*32*). Therefore, the incorporation of Aib into a polypeptide chain is expected to indirectly stabilize the folded structure by decreasing the chain entropy of the unfolded state. This principle has been previously proposed and experimentally verified by exchanging Gly with Ala in proteins (*33*−*35*). In fact, both Gly → Ala and Ala → Aib replacements introduce at the C_α atom an extra methyl group that greatly reduces the possible conformations of the peptide chain in the unfolded state, thus shifting the equilibrium to the folded state (*33*). In this respect, it is of interest to observe that the hydrogen-bonding pattern characteristic of the helical structure in some Aib-rich short peptides does not appear to be fully disrupted up to 150 °C, reflecting the absence of any true unfolded conformation of the peptide chain even at extreme temperatures (*36*).

The aim of the present work is to investigate the effects of Aib on the structure and stability of a globular protein. As a model system, we choose the C-terminal fragment 255−316 of thermolysin, a heat-stable metalloprotease of known 3D structure (*37*) that has for many years been utilized in our laboratory as a model protein for studying various aspects of protein structure, folding, and stability properties. We have demonstrated previously that the proteolytic fragment 255−316 of thermolysin possesses domain-like characteristics, since it is able to fold into a stable, native-like structure (*38*). Two-dimensional NMR measurements showed that the solution structure of fragment 255−316 consists of a symmetric dimer formed by two subunits each containing three helical segments spanning residues 260−274, 281−295, and 301−311 (39) (see Figure 1A,B) and that the global fold of each monomer is largely coincident with that of the corresponding region in the X-ray structure of thermolysin (*37*). Of interest, the interface between the two subunits of the fragment dimer is of marked hydrophobic character and coincides topologically with that between fragment 255−316 and the rest of the protein in the intact protein. Differential scanning calorimetry (DSC) measurements indicated that fragment 255−316 behaves as a highly stable dimer, undergoing a reversible two-state thermal unfolding process characterized by thermodynamic parameters similar to those normally observed for small globular proteins (*40*).

The incorporation of Aib into the thermolysin subdomain 255−316 was achieved by enzymatic coupling of fragment 255−302 to Aib-containing synthetic analogs of peptide 303−316 using V8-protease in 50% (v/v) aqueous glycerol (*41*). Depending upon the location of the Aib exchange along the polypeptide chain of fragment 255−316, the Aib residue was found to stabilize the folded conformation of the fragment to a different extent. The physicochemical determinants of protein stabilization and the possible molecular mechanisms responsible for the context-dependent effects of the Ala → Aib substitutions are discussed.

MATERIALS AND METHODS

Materials. Thermolysin (EC 3.4.24.27) from *Bacillus thermoproteolyticus* and subtilisin Carlsberg (EC 3.4.21.14) from *Bacillus subtilis* were purchased from Sigma (St. Louis, MO), while V8-protease from *Staphylococcus aureus* (EC 3.4.21.19) was from Boehringer (Mannheim, Germany). Protected amino acids, solvents, and reagents for peptide synthesis, as well as those for peptide/protein sequence analysis, were purchased from Applied Biosystems (Foster City, CA). Trifluoroacetic acid (TFA) and phenyl isothiocyanate (PITC) were obtained from Pierce (Rockford, IL), while ethanedithiol (EDT), glycerol, and ethylenediaminetetraacetic acid sodium salt (EDTA) were from Fluka (Basel, Switzerland). All other reagents and organic solvents were of analytical grade and obtained from Fluka or Merck (Darmstadt, Germany).

Preparation of Fragments 255−*316 and 255*−*302*. The semisynthetic approach for preparing Aib-containing analogs of the thermolysin C-terminal fragment 255−316 involves the enzymatic coupling of fragment 255−302 to synthetic Aib analogs of peptide 303−316. Fragment 255−302 was prepared from the full-length thermolysin chain by a series of proteolytic reactions leading to truncation of the 316-residue chain of thermolysin as follows: 1−316 → 205−316 → 255−316 → 255−302. The thermolysin fragment 255−316 was prepared by subjecting the larger fragment

[1] Abbreviations: standard three-letter abbreviations are used for all natural amino acids; Aib, α-aminoisobutyric acid; ASA, accessible surface area; Boc, *tert*-butyloxycarbonyl; CD, circular dichroism; CZE, capillary zone electrophoresis; DSC, differential scanning calorimetry; EDT, ethanedithiol; EDTA, ethylenediaminetetraacetic acid; Fmoc, 9-fluorenylmethyloxycarbonyl; Gdn·HCl, guanidine hydrochloride; HBTU, 2-(1*H*-benzotriazol-1-yl)-1,1,3,3-tetramethyluronium hexafluorophosphate; HOBt, 1-hydroxybenzotriazole; HPLC, high-pressure liquid chromatography; NMP, *N*-methylpyrrolidone; PTC, phenylthiocarbamoyl; PTH, phenylthiohydantoin; RP, reverse-phase; SDS, sodium dodecyl sulfate; TFA, trifluoroacetic acid; T_m, melting temperature; UV, ultraviolet; v/v, volume to volume; w/w, weight to weight; Ala304Aib, Ala309Aib, and Ala312Aib refer to thermolysin fragment 255−316 with a single Ala residue replaced by Aib at the specified position; Ala304Aib/Ala309Aib refers to fragment 255−316 in which Ala304 and Ala309 have both been replaced by Aib.

205−316, obtained by autolysis of thermolysin in the presence of EDTA (*42*), to limited proteolysis with subtilisin following essentially the procedure previously reported for the BrCN fragment 206−316 (*38*). Fragment 205−316 (2 mg/mL) was digested with subtilisin at room temperature (22−24 °C) for 3.5 h in 20 mM Tris·HCl−0.1 M NaCl, pH 9.0, using a protease to substrate ratio of 1:200 (w/w). Proteolysis was stopped by adding formic acid up to 10% (v/v), and then the 62-residue fragment 255−316 was purified on a Sephadex G-50 gel filtration column eluted with 5% (v/v) formic acid. The peptide material of the major chromatographic peak was collected, lyophilized, and further purified by preparative RP-HPLC.

Thermolysin fragment 255−302 was prepared by proteolytic cleavage of fragment 255−316 at the level of the single Glu302 of the polypeptide chain using the Glu-specific V8-protease from *Staphylococcus aureus* (*43*). The reaction was carried out at room temperature for 24 h in 0.1 M ammonium bicarbonate buffer (10 mL), containing 1 mM EDTA and 0.2% SDS, at a peptide concentration of 2 mg/mL and using a protease:peptide ratio of 1:20 (w/w). After the proteolytic reaction was complete, SDS was precipitated by adding 500 μL of a 7 M Gdn·HCl solution to the reaction mixture. This procedure was found to effectively remove SDS from the solution (see *41*, for more details). After centrifugation, fragment 255−302 was purified to homogeneity by preparative RP-HPLC. The fragment thus obtained was tested for purity and identity and subsequently employed in the enzyme-catalyzed semisynthetic procedure.

Peptide Synthesis. Aib-containing analogs of the C-terminal peptide 303−316 of thermolysin were synthesized by the solid-phase Fmoc method (*44*) using a Model 431A Applied Biosystems peptide synthesizer. The peptide chain was assembled stepwise on a *p*-alkoxybenzyl ester polystyrene resin cross-linked with 1% divinylbenzene (0.1 g) (*45*) and derivatized with Fmoc-Lys (0.5 mequiv/g). The *tert*-butyloxycarbonyl (Boc) side-chain protecting group was used for Lys, *tert*-butyl (*t*Bu) for Ser and Asp, and triphenylmethyl (Trt) for Gln. Coupling reactions were performed with the HBTU/HOBt activation procedure (*46*) according to the FastMoc protocol (Applied Biosystems User Bullettin no. 30, 1990) and using a 10-fold molar excess of Nα-Fmoc-protected amino acids. In order to increase the yield of the coupling reaction, a double coupling cycle was used for Aib and for the amino acid residue at the Aib + 1 position (*47*). After peptide assembly was completed, the side-chain protected peptidyl resin (0.25 g) was treated for 90 min at 0 °C with a 10-mL mixture of TFA/H_2O/EDT (90:5:5, v/v) to cleave the peptide from the resin and to remove the side-chain protecting groups. The crude peptide was purified by preparative RP-HPLC and checked for homogeneity and identity.

Semisynthesis. The enzyme-catalyzed coupling of the thermolysin fragment 255−302 to the synthetic Aib-containing analogs of peptide 303−316 was conducted following essentially the procedure described previously for fragment 205−316 (*41*). The natural fragment 255−302 was dissolved (1 mg/mL, ∼0.2 mM) in 0.1 M ammonium acetate buffer (0.2 mL), pH 6.4, containing 50% (v/v) glycerol, in the presence of 5-fold molar excess of synthetic peptide analog 303−316, and the enzymatic coupling was started by adding 2 μL of a stock solution (2 mg/mL) of V8-protease at an enzyme to fragment 255−302 ratio of 1:50 (w/w). The semisynthetic reaction was carried out in the dark at room temperature for 5−7 days, and then the mixture was diluted 10-fold with 0.05% aqueous TFA in order to stop the reaction. The mixture was fractionated by RP-HPLC using an Aquapore RP-300 C8 column (4.6 × 100 mm, 7 μm) (Brownlee Labs, Santa Clara, CA). The Aib-containing analogs of fragment 255−316 thus obtained were analyzed for their purity, chemical identity, and conformational and stability properties.

Analytical Methods. Amino acid analyses were performed by using the Pico-Tag method (Millipore-Waters, Milford, MA) (*48*). Of note, the reaction of PITC with Aib led to a product eluted from the Pico-Tag column at shorter retention time (8 min, after PTC-Pro), corresponding to PTC-Aib, as well as to a second component, eluted at longer retention time (18 min, after PTC-Lys), corresponding to the cyclic phenylthiohydantoin(PTH)-Aib derivative (5,5-dimethyl-3-phenyl-2-thiohydantoin). Standards of these two Aib derivatives were prepared by reacting Aib with PITC, and their chemical identity was verified by ultraviolet (UV), infrared (IR), and ^{1}H-NMR spectroscopy (not shown). It was observed that after 2 h incubation in the sample diluent (5 mM sodium phosphate buffer, pH 6.0, containing 5% acetonitrile) PTC-Aib was quantitatively converted into the cyclic PTH-Aib, since the *gem*-dimethyl group at Cα atom greatly enhances the rate of cyclization of the PTC derivative of the amino acid (unpublished results). The chromatograhic peak of the PTH-Aib was used to quantitate the Aib content in the amino acids hydrolysates.

N-Terminal sequence analysis was performed with an Applied Biosystems peptide/protein sequencer, Model 477A, equipped with on-line PTH-analyzer, Model 120A. Standard manufacturer's procedure and programs were used with minor modifications.

Capillary zone electrophoresis (CZE) was performed on a Bio-Rad (Richmond, CA) instrument, Model HPE-100, utilizing a fused silica capillary (50 μm × 35 cm). Samples were dissolved (1 mg/mL) in 0.1 M phosphate buffer, pH 3.5, and injected onto the capillary by applying an electric field of 10 kV for 6 s. The electrophoretic separation was carried out at room temperature, applying an electric field of 300 V/cm, and the absorbance of the effluent was monitored at 200 nm.

Electrospray mass spectrometry analyses were performed using a PE-SCIEX (Thornhill, Ontario, Canada) single quadrupole (API-1) mass spectrometer equipped with a nebulization-assisted electrospray ionization source. Samples (10−20 pmol/μL) were injected into the spectrometer at a flow rate of 4 μL/min. Scans were taken in the positive ion mode over the *m/z* range of 400−1600. Mass calibration was carried out using horse heart myoglobin (Sigma) as an external standard. The results of mass spectrometry measurements were in agreement with theoretical data: natural fragment 255−316, found 6624.0 Da (calculated 6624.5); Ala304Aib, 6638.0 (6638.5); Ala309Aib, 6637.2 (6638.5); Ala312Aib, 6638.0 (6638.5); Ala304Aib/Ala309Aib, 6652.1 (6652.5).

Spectroscopic Measurements. Peptide/protein concentrations were determined by ultraviolet (UV) absorption measurements at 280 nm on a double beam model Lambda-2 spectrophotometer from Perkin-Elmer (Norwalk, CT). Ex-

tinction coefficients (mg^{-1}·cm^2) of protein fragments were calculated at 280 nm (*49*) and taken as 1.52 for intact thermolysin, 0.86 and 0.735 for fragments 205−316 and 255−302, respectively, and 0.58 for fragment 255−316 and its Aib derivatives.

Circular dichroism (CD) spectra were recorded on a Jasco (Tokyo, Japan) Model J-710 spectropolarimeter equipped with a thermostated cell-holder and a Neslab (Newington, NH) Model RTE-110 water circulating bath. The instrument was calibrated with *d*-(+)10-camphorsulfonic acid (50). Far- and near-UV CD spectra were taken at 25 °C in 20 mM sodium phosphate buffer, pH 7.5, containing 0.1 M NaCl at a fragment concentration of 50−80 μM and using 0.2- or 10-mm path length quartz cells in the far- and near-UV region, respectively. The results were expressed as the mean residue ellipticity, $[\theta]_{MRW} = (\theta_{obs}/10)(MRW/lc)$, where θ_{obs} is the observed ellipticity in degrees at a given wavelength, MRW is the mean residue weight taken as 107 Da for the natural and semisynthetic analogs of fragment 255−316, l is the cuvette pathlength in centimeters, and c is the fragment concentration in grams per milliliter.

Thermal Unfolding. The heat-mediated unfolding of Aib-containing analogs and natural fragment 255−316 of thermolysin was followed by recording the decrease of the CD signal at 222 nm as a function of the sample temperature. The fragment was dissolved (4.5 μM) in 20 mM sodium phosphate buffer, pH 7.5, containing 0.1 M NaCl, and placed in a 1-cm path length cuvette, which was heated (under stirring) at a linear heating rate of 50 °C/h. Samples were prepared by diluting aliquots (100−200 μL) of concentrated stock solution (70−140 μM) with phosphate buffer to a final volume of 3 mL. Both CD signal and temperature data were recorded simultaneously by a computer program provided by Jasco. The reversibility of the thermal unfolding process was determined by measuring the recovery of the CD signal upon cooling to the initial temperature (20 °C).

Thermal denaturation transition curves were analyzed within the framework of the two-state model assuming that the native dimer (N_2) unfolds to denatured monomers (U), according to the scheme $N_2 \leftrightarrow 2U$ previously established for the natural fragment 255−316 by calorimetric measurements (*40*). At a given temperature, only native, f_N, and unfolded, f_U, fractions of fragment molecules are present at significant concentration, so that $2f_N + f_U = 1$. The fraction of unfolded molecules, f_U, was calculated as $f_U = ([\theta]_{222} - [\theta]_N)/([\theta]_U - [\theta]_N)$, where $[\theta]_{222}$ is the observed ellipticity at 222 nm at a given temperature and $[\theta]_N$ and $[\theta]_U$ represent the ellipticity values at 222 nm of native and unfolded states at that temperature, respectively. At each temperature in the range 20−90 °C, $[\theta]_N$ and $[\theta]_U$ were calculated from the linear extrapolation of the unfolding data in the pre- and posttransition region, respectively. The melting temperature, T_m, defined as the temperature at which the molar fraction of unfolded molecules is 0.5, was derived from the linear regression equation obtained by plotting f_U *vs* T in the transition region. Given [P] is the total molar concentration of fragment expressed in monomer units, it is possible to derive for each temperature in the transition region the equilibrium constant, $K_U = [U]^2/[N_2] = 2[P][(f_U)^2/(1 - f_U)]$, and the free energy change, $\Delta G_U = -RT \ln K_U$, for the unfolding reaction, where R is the gas constant (1.987 cal·mol^{-1}·K^{-1}) and T is the absolute temperature. It is noteworthy that, for a dimeric protein following a two-state $N_2 \leftrightarrow 2U$ unfolding process, the equilibrium constant at T_m, $K_U(T_m)$, is equal to [P] and hence $\Delta G_U(T_m) = -RT \ln [P]$. The difference in free energy change ($\Delta\Delta G_U$) between the conformational stability of the Aib-containing analogs 255−316, $\Delta G_{U,Aib}$, and that of the natural fragment 255−316, $\Delta G_{U,wt}$, was calculated at the melting temperature of the natural species ($T_{m,wt}$). The unfolding free energy changes for Ala304Aib and Ala312Aib analogs of fragment 255−316 were calculated using values of K_U measured at $T_{m,wt}$. In fact, $T_{m,wt}$ is within the temperature interval in which ΔG_U for Ala304Aib and Ala312Aib can be approximated as a linear function of temperature (*51*), and thus $\Delta\Delta G_U$ can be calculated directly from the equation $\Delta\Delta G_U = -RT \ln (K_{U,Aib}/K_{U,wt})$. In the case of Ala309Aib and the doubly substituted Ala304Aib/Ala309Aib analog, which are substantially more stable than the natural species (see Results), the value of $T_{m,wt}$ is out of the temperature range where ΔG_U for these analogs can be considered linearly related to T. Therefore, the unfolding free energy changes for Ala309Aib and the doubly substituted Ala304Aib/Ala309Aib analog were calculated at $T_{m,wt}$ according to the van't Hoff equation $\Delta G_{U,Aib}(T_{m,wt}) = \Delta H_{m,Aib}[1 - (T_{m,wt}/T_{m,Aib})] - \Delta C_p[(T_{m,Aib} - T_{m,wt}) + T_{m,wt} \ln (T_{m,wt}/T_{m,Aib})] - RT_{m,Aib}[P]_{Aib}$, where $T_{m,Aib}$ and $[P]_{Aib}$ are the melting temperature and the molar concentration of Aib derivatives, respectively, ΔC_p is the heat capacity change ($\Delta C_p = C_{p,U} - C_{p,N}$) of the unfolding reaction at constant pressure, and $\Delta H_{m,Aib}$ is the unfolding enthalpy change calculated at $T_{m,Aib}$. The value of ΔC_p used here for Aib analogs was that obtained by calorimetric measurements conducted on the natural fragment 255−316, taken as 0.6 ± 0.1 kcal·mol^{-1}·K^{-1} (*40*) and assumed to be constant over the temperature range 20−80 °C (*51*, *52*). $\Delta H_{m,Aib}$ was calculated according to the equation $\Delta H_m = \Delta G_m + T_m\Delta S_m$, where ΔG_m and T_m are determined as reported before and ΔS_m can be calculated from the plot of $\Delta G_{U,Aib}$ *vs* T, using the equation $\Delta S_{m,Aib} = -d\Delta G(T_{m,Aib})/dT$.

Model Building. The 3D model of Aib-containing analogs was based on the NMR structure of the thermolysin domain 255−316 (PDB entry code 1TRL; *39*) and was obtained by replacing Ala residue(s) for Aib at the desired position without additional molecular dynamics relaxation. The model was built using the program Insight-II (Biosym Technologies, La Jolla, CA) run on a Silicon Graphics IRIS SD/35 workstation. Accessible surface area (ASA) calculations were carried out by using the program ACCESS (*53*) and using a probe radius of 1.4 Å.

RESULTS

Semisynthesis of Aib Analogs of Fragment 255−316. The Aib-containing analogs of the carboxy-terminal subdomain 255−316 of thermolysin were obtained by enzyme-catalyzed coupling of fragment 255−302 to each of the synthetic peptide analogs of fragment 303−316 in which Ala → Aib exchanges have been introduced at the desired position(s) (see Figure 1C).

The natural fragment 255−302 was obtained by two steps of proteolysis of the larger fragment 205−316, which in turn was produced in high yields by EDTA-mediated autolysis of thermolysin (*42*). In the presence of 10 mM EDTA, the

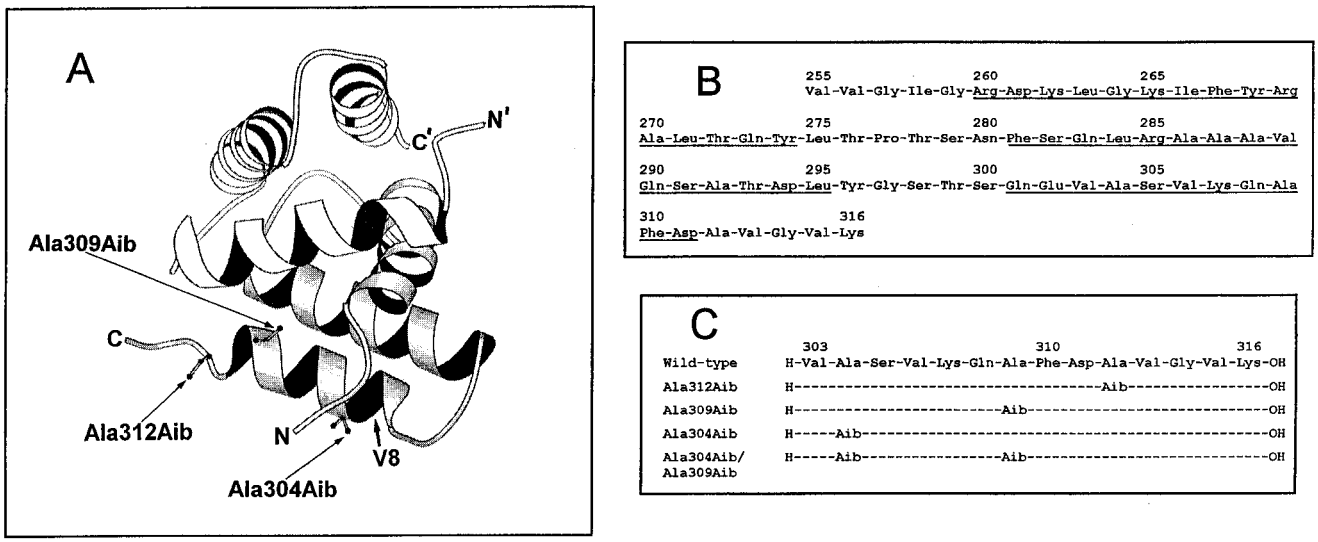

FIGURE 1: (A) Schematic representation of the dimeric 3D structure of the C-terminal domain 255−316 of thermolysin, as given by NMR analysis (*39*). For clarity, the locations of the Aib residue in positions 304, 309, and 312, shown in ball-and-stick representation, are indicated for only one monomer. N, N′ and C, C′ indicate the NH_2- and COOH-termini of the two monomers. The arrow indicates the site of cleavage by V8-protease at the single Glu302. The ribbon drawing was generated using the program MOLSCRIPT (*88*). (B) Amino acid sequence of the C-terminal domain 255−316 of thermolysin (*89*). Residues comprised in helical segments are underlined. The assignment of secondary structure elements is that reported for the NMR solution structure of the dimeric form of fragment 255−316 (*39*). (C) Amino acid sequence of the thermolysin peptide 303−316 and of its Aib-containing analogs obtained by solid-phase synthesis.

less tightly bound calcium ion (Ca-4) is removed from the protein, causing a local unfolding of the calcium-binding loop that becomes susceptible to proteolytic attack by the active thermolysin molecules still present in solution. In a subsequent step, limited proteolysis of fragment 205−316 with subtilisin led to the folded and stable C-terminal domain 255−316 (*38*), suggesting that the N-terminal region of fragment 205−316 (about 50 amino acids) is largely unfolded and thus susceptible to proteolysis, as recently verified by NMR (M. Rico, personal communication) and calorimetric (*54*) analyses. Subsequently, fragment 255−316 was selectively and quantitatively cleaved in slightly denaturing conditions (0.2% SDS or 4 M urea) by the Glu-specific V8-protease from *Staphylococcus aureus* at the level of the single Glu302 located at the first turn of the C-terminal helix (Figure 1A,B), leading to the formation of fragments 255−302 and 303−316. At variance from the parent fragment 255−316, both proteolytic fragments 255−302 and 303−316 were found to be essentially unfolded by CD spectroscopy (not shown), indicating that the removal of the C-terminal helix disrupts the native-like fold of the protein subdomain 255−316.

The Aib-containing analogs of the 14-residue peptide 303−316 were synthesized by automated stepwise solid-phase synthesis utilizing Fmoc-chemistry (*44*) and the HBTU/HOBt activation procedure (*46*) on a *p*-alkoxybenzyl ester resin. Due to the steric hindrance of the methyl groups on the C_α atom, the coupling efficiencies of Aib and of the residue at the Aib + 1 position in the stepwise assembly of the peptide chain are usually poor (*55*). To overcome this problem, several new carboxyl-activating agents have been recently proposed (*56*). In our case, a double coupling cycle with HBTU/HOBt was used for Aib and for the amino acid just following the Aib residue on the growing peptide chain. As a result, both Ala309Aib and Ala312Aib analogs of fragment 303−316 were obtained in high yields (up to 90%). Conversely, the analog Ala304Aib of fragment 303−316, as well as the doubly substituted derivative Ala304Aib/Ala309Aib, was obtained with a ∼35% yield. The chemical characterization of the synthetic mixtures led to the conclusion that the low yields of synthesis for these peptide analogs are determined by the poor efficiency of the covalent coupling between the sterically hindered residues Val303 and Aib304. All Aib-containing derivatives of peptide 303−316 were isolated to homogeneity by micropreparative RP-HPLC, and their identity was established by amino acid analysis after acid hydrolysis (not shown) and mass spectrometry (see Materials and Methods).

The restitching of fragments 255−302 and 303−316 by the use of V8-protease was achieved by following essentially the procedure previously developed for the semisynthesis of the larger fragment 205−316 (*41*). The natural fragment 255−302 was allowed to react with a 5-fold molar excess of synthetic Aib analog of fragment 303−316 (see Figure 1C) in 0.1 M ammonium bicarbonate buffer, pH 6.0, containing 50% (v/v) glycerol as organic cosolvent, in the presence of V8-protease (see Materials and Methods). The time course of the enzyme-catalyzed synthesis was followed by RP-HPLC analysis. As an example, Figure 2 shows the RP-HPLC profile of the semisynthetic reaction of fragment 255−302 with the synthetic Aib-peptide 303−316, with the Ala → Aib exchange in position 309 of the chain, before (Figure 2A) and after 5-days incubation (Figure 2B) with V8-protease. Upon addition of the protease, a new component was generated in the mixture eluting from the HPLC column after fragment 255−302, whereas the amount of this latter component was significantly reduced (Figure 2B). The peptide products of semisynthesis were purified by micropreparative HPLC and analyzed for their purity and identity. The homogeneity of the semisynthetic analogs was assessed by analytical RP-HPLC and capillary zone electrophoresis (CZE) (not shown), while the chemical identity was established by analyzing their amino acid composition after acid hydrolysis and by electrospray ionization (ESI) mass spec-

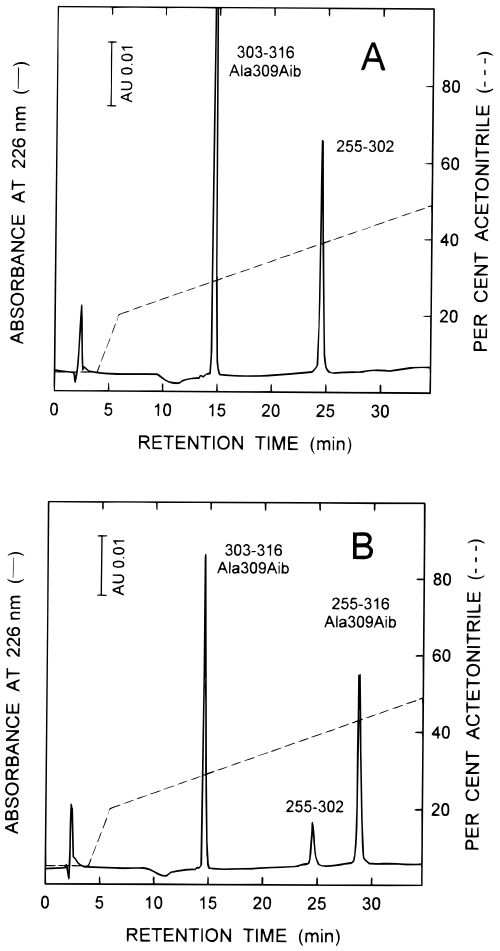

FIGURE 2: RP-HPLC analysis of the V8-protease-mediated coupling of natural fragment 255−302 to the synthetic peptide 303−316 with Ala → Aib exchange in position 309 before (A) and after (B) 5-days reaction. An aliquot (100 μg) of the reaction mixture was applied to an Aquapore RP-300 C8 column (4.6 × 100 mm), which was eluted at a flow rate of 0.8 mL/min with a linear gradient (- - -) of acetonitrile in 0.05% (v/v) aqueous TFA. Numbers near the chromatographic peaks refer to the identity of the peptide material eluted from the column.

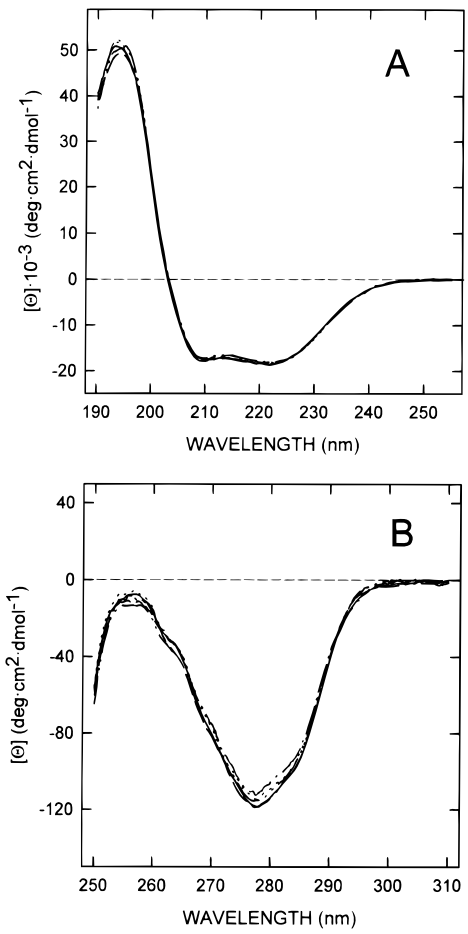

FIGURE 3: Far- (A) and near-UV (B) CD spectra of the C-terminal domain 255−316 of thermolysin (—) and of its semisynthetic analogs Ala304Aib (- - -), Ala309Aib (—·—), Ala312Aib (···), and Ala304Aib/Ala309Aib (—··—). Spectra were taken at 25 °C in 20 mM sodium phosphate buffer, pH 7.5, containing 0.1 M NaCl at a fragment concentration of 50−80 μM and using a 0.2- or 10-mm path length cuvette in the far- and near-UV region, respectively.

trometry (MS). Both amino acid analysis and ESI-MS data are in agreement with those calculated from the amino acid sequence of the various fragments. Moreover, the results of automated N-terminal sequence analyses (not shown) further confirmed the chemical identity of the purified semisynthetic Aib fragments.

The V8-protease-mediated coupling of all the Aib analogs proceeded in high yields (up to 90%), similar to those observed when fragment 205−302 was coupled to the natural peptide 303−316, indicating that the coupling efficiency is not affected by the presence of Aib residue(s) along the peptide sequence. Thus, the semisynthetic procedure allowed us to prepare the Aib analogs of fragment 255−316 in sufficient quantity and high purity for conducting the conformational and stability studies reported below.

Conformational Characterization of Aib Analogs. The conformational properties of the Aib analogs of fragment 255−316 were investigated by circular dichroism (CD) spectroscopy in the far- (Figure 3A) and near-UV (Figure 3B) region. The far-UV CD spectra show the presence of two minima at 222 and 208 nm and a maximum at 193 nm, characteristic of a polypeptide chain possessing a high α-helix content (*57*). The near-UV CD is dominated by the negative absorption of tyrosines centered at 278 nm, while some phenylalanine fine structure is visible in the 260−270 nm region (*58*). Interestingly, the CD spectra of the Aib derivatives in the far- and near-UV region are superimposable to each other and very similar to those of the natural fragment, indicating that both the helical secondary structure (far-UV CD) as well as the aromatic side-chain topology (near-UV CD) of the protein domain 255−136 are fully retained upon Ala → Aib replacement(s). It should be emphasized that near-UV CD is a very sensitive probe of protein conformation, so that even small perturbations of tertiary structure can dramatically alter the resulting CD spectrum (*58*, *59*). Therefore, the identity of the near-UV CD spectra for all Aib analogs (see Figure 3B) is taken as strong evidence that the incorporation of Aib residue(s) into fragment 255−316 does not perturb its native three-dimensional structure.

Stability Properties of Aib Analogs. The thermal unfolding of the natural fragment 255−316 and of its Aib derivatives was followed by monitoring the temperature dependence of the dichroic signal at 222 nm, which is a sensitive parameter of the helical secondary structure (Figure 4). The unfolding process of either natural or semisynthetic analogs is highly cooperative, as judged from the sigmoidal shape of the

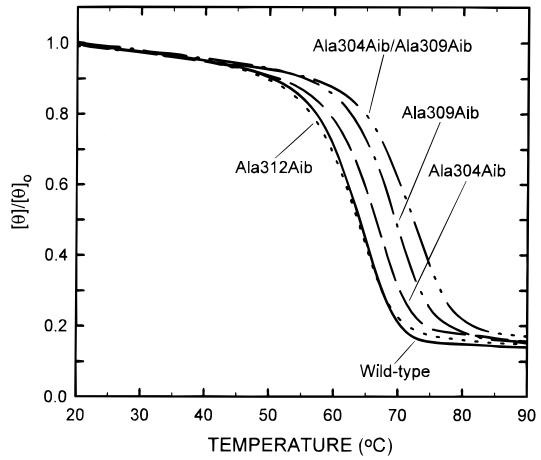

FIGURE 4: Thermal unfolding of the natural fragment 255−316 and of its semisynthetic Aib derivatives. Denaturation experiments were carried out at a protein concentration of 4.5 μM (~30 μg/mL) in 20 mM sodium phosphate buffer, pH 7.5, containing 0.1 M NaCl, using a 1-cm path length cuvette heated at a linear heating rate of 50 °C/h. The unfolding process was monitored by CD changes at 222 nm, and data are reported as the ratio $[\theta]/[\theta]_o$, where $[\theta]_o$ is the ellipticity value at the initial temperature (20 °C). (—) Natural fragment 255−316; (- - -) Ala304Aib; (—·—) Ala309Aib; (···) Ala312Aib; (—··—) Ala304Aib/Ala309Aib.

thermal transition curves, and fully reversible (at least 95%) upon lowering the temperature to the initial value (20 °C).

Previous differential scanning calorimetry (DSC) measurements allowed us to calculate the thermodynamic quantities characterizing the thermal unfolding of the natural fragment 255−316 (*40*). It was concluded that this fragment behaves as a dimer in solution, undergoing a two-state reversible thermal unfolding process according to the scheme $N_2 \leftrightarrow 2U$ (*40*). On this basis, the thermal transition curves shown in Figure 4 were treated within the framework of a two-state model, in which the folded dimer (N_2) unfolds into two denatured monomers (U). At a given temperature, only native, f_N, and unfolded, f_U, fractions of protein molecules are present at significant concentration, so that $2f_N + f_U = 1$. The melting temperature, T_m, defined as the temperature at which the molar fraction of unfolded molecules is 0.5, and the difference in the unfolding free energy change ($\Delta\Delta G_U$) were calculated from the thermal unfolding curves. The data reported in Table 1 clearly indicate that the effects of Ala → Aib substitution are remarkably context-dependent, since the same mutation at different sites causes different stabilizing effects. In particular, the Ala → Aib substitution in position 304 enhances the thermal stability of the protein domain by 2.2 °C, as estimated by the difference in T_m of the Aib analog with respect to that of the natural Ala-containing fragment. This stabilizing effect is even more pronounced when Ala309 is replaced by the Aib residue ($\Delta T_m = +5.4$ °C). Surprisingly, the protein domain is slightly destabilized ($\Delta T_m = -0.6$ °C) by Ala → Aib replacement in position 312. When Aib was introduced at both positions 304 and 309, the dimeric structure of the fragment was stabilized by 8.0 °C. Interestingly, the stabilizing effects of these replacements are nicely additive, if compared to the singly-substituted analogs, in terms of both ΔT_m and $\Delta\Delta G_U$ (Table 1).

Table 1: Thermodynamic Data for the Thermal Unfolding of Natural Fragment 255−316 and Its Semisynthetic Aib Analogs[a]

fragment 255−316	T_m[b] (°C)	ΔT_m[c] (°C)	$\Delta\Delta G_U$[d] (kcal·mol^{-1})
natural fragment	63.5	–	–
Ala312Aib	62.9	−0.6	−0.20
Ala304Aib	65.7	2.2	0.71
Ala309Aib	68.9	5.4	1.76
Ala304Aib/Ala309Aib	71.5	8.0	2.43

[a] The thermodynamic parameters were obtained by analyzing the thermal denaturation curves reported in Figure 4 within the framework of a two-state model, $N_2 \leftrightarrow 2U$, previously established for the natural species by calorimetric measurements (*40*). [b] T_m is the melting temperature, defined as the temperature at which the molar fraction of unfolded molecules is 0.5. The data reported results from the average of heat-induced denaturation experiments conducted in triplicate. The error on the estimation of T_m is ±0.2 °C or less. [c] ΔT_m is the change in melting temperature of the Aib analog relative to the natural fragment. [d] $\Delta\Delta G_U$ is in monomer units and is the difference between the free energy of unfolding of each Aib analog and that of natural fragment 255−316 at the melting temperature of the wild-type species, $T_{m,wt}$. $\Delta\Delta G_U$ values are calculated as reported under Materials and Methods. A positive value of $\Delta\Delta G_U$ indicates that the Aib analog is more stable than the wild-type fragment. The error on the determination of free energy changes was approximately 10%.

DISCUSSION

Semisynthesis of Fragments. The semisynthetic approach described here for preparing analogs of the C-terminal domain of thermolysin is both practical and useful. The addition of the organic cosolvent glycerol significantly favors synthesis over hydrolysis of peptide bonds by V8-protease, and the restitching of fragments 255−302 and 303−316 occurs in remarkable high yields (~90%, after 5−7 days of reaction), in analogy to those previously reported for the longer fragment 205−316 (*41*). Enzyme-catalyzed semisynthesis allows incorporation of noncoded amino acids or site-specific labels into large polypeptides or even proteins with minimum chemical handling and without the undesirable side products usually generated in the chemical synthesis. However, a semisynthetic procedure is usually complicated by the fact that the protease used for the synthesis often degrades the end product of the reaction and thus the yields of the final semisynthetic product are poor. The high yields of the present system can be explained by proposing that the semisynthetic fragment is quite resistant to proteolysis and slowly accumulates in the reaction mixture. Indeed, the folded fragment 255−316 in aqueous buffer is not degraded by V8-protease, and its single site of possible proteolytic attack, the peptide bond Glu302−Val303, is cleaved by the Glu-specific V8-protease only if the fragment is (partly) denatured in the presence of 4 M urea or 0.2% SDS (see Materials and Methods).

The solid-phase chemical synthesis of Aib analogs of the thermolysin peptide 303−316 required a double coupling cycle for the incorporation of Aib and of the amino acid residue at the Aib+1 position, as expected by considering the steric hindrance of the Aib residue. Using this treatment, the yields of the final synthetic peptide were quite high (~90%), but were much lower (~35%) for the peptide analogs requiring peptide bond formation between two sterically hindered amino acid residues, such as the peptide bond between Val303 and Aib304 (see Results). These observations indicate that the total chemical synthesis of Aib analogs of the 62-residue fragment 255−316 likely would

Table 2: Backbone Dihedral Angles (ϕ, ψ)[a] and Solvent-Accessible Surface Areas (A)[b] of Ala and Aib at Positions 304, 309, and 312 of Thermolysin Domain 255−316

Ala											
304				309				312			
ϕ (deg)	ψ (deg)	A_ϕ (Å^2)	ΔA_ϕ (Å^2)	ϕ (deg)	ψ (deg)	A_ϕ (Å^2)	ΔA_ϕ (Å^2)	ϕ (deg)	ψ (deg)	A_ϕ (Å^2)	ΔA_ϕ (Å^2)
-55 ± 3	-47 ± 4	30	35	-57 ± 3	-46 ± 4	0	65	-90 ± 14	10 ± 20	25	40

Aib					
304		309		312	
A_ϕ (Å^2)	ΔA_ϕ (Å^2)	A_ϕ (Å^2)	ΔA_ϕ (Å^2)	A_ϕ (Å^2)	ΔA_ϕ (Å^2)
45	65	0	110	40	70

[a] Average values of ϕ and ψ at each position are reported together with the corresponding root mean square deviations calculated on the eight final structures of the two subunits in the dimeric fragment 255−316 (39). ϕ and ψ values of Aib residues are those measured for Ala at the corresponding position in the natural fragment. [b] Accessibility values are based on the NMR solution structure of dimeric fragment 255−316 (*39*). Solvent-accessible surface areas are obtained using the program ACCESS (*53*) and are reported as the average value *per* monomer unit. Accessibility values of Aib analogs are inferred from model building by replacing Ala for Aib at the specified position, without additional molecular refinement. A_ϕ is the hydrophobic surface area of Ala or Aib side chains accessible to solvent in the folded state. $\Delta A_\phi = A_{\phi,U} - A_\phi$ represents the difference in solvent exposure of Ala or Aib side chains in the unfolded ($A_{\phi,U}$) and folded (A_ϕ) state. The unfolded state is approximated by the tripeptide Gly-X-Gly in the extended conformation ($\phi = -120°$, $\psi = +140°$) (*87*). $A_{\phi,U}$ values were calculated as 65 and 110 Å^2 for Ala and Aib, respectively.

be unpractical, considering that the overall yields of the desired fragment would be prohibitively low.

Protein Stability. The structural features of mutated proteins obtained by chemical or genetic methods, relative to those of the wild-type species, are critical for a correct interpretation of protein engineering experiments. In fact, if the structural consequences of a mutation at a given site are known to be restricted to the local environment in which the mutation has been introduced, while the overall protein fold is unchanged, then it is possible to use a "minimalist approach" (*60*) in interpreting stability or functional changes in mutant proteins and to ascribe the observed differences in the properties of the mutant exclusively as deriving from the modified side chain only. The results of the conformational characterization of the semisynthetic Aib analogs, conducted by far- and near-UV CD measurements, allow us to firmly establish that the secondary structure as well as the side chain packing of the native species is retained upon Ala → Aib replacement(s). On this basis, the observed changes in stability of the Aib analogs can be related solely to the effects of the Ala → Aib exchange at specific locations along the polypeptide chain of the fragment. However, the possibility that Ala → Aib substitutions can affect the dimerization constant and hence the overall stability of the dimer should also be taken into account. This possibility cannot be ruled out for the Ala309Aib analog, since Ala309 is in a hydrophobic environment close to the dimer interface (see Figure 1). Conversely, both Ala304 and Ala312 are solvent-exposed, far from the dimerization interface, and hence it is unlikely that Ala → Aib substitutions at these positions could change the stability of the dimer by altering the interactions between the two monomers. In the following, we will attempt to understand the physical basis of Aib-mediated protein stabilization by quantitating the impact of amino acid substitution(s) on the free energies of the folded and the unfolded forms of the dimeric fragment 255−316 in terms of side-chain and backbone entropy, hydrophobicity, and strain energy changes caused by the Ala → Aib replacement(s). The stability data were interpreted on the basis of the 3D model, obtained by replacing Ala residue(s) for Aib at the desired position in the NMR solution structure of the dimeric fragment 255−316 (*39*).

Ala304Aib. The Ala304 residue is located at the end of the first turn of the C-terminal helix 301−311 and is solvent-exposed (*39*). The backbone conformational angles of Ala304 ($\phi = -55° \pm 3°$ and $\psi = -47° \pm 4°$, see Table 2) are within the range allowed to the rather fixed geometry of Aib ($\phi = \pm 57°$ and $\psi = \pm 47°$) (*30*), suggesting that no strain has been introduced upon Ala → Aib substitution. In addition, model building and ASA calculations indicate that position 304 can potentially accommodate the extra β'-carbon of Aib without significantly interfering with neighboring atoms. As a result, the substitution of Ala304 for Aib enhances the thermal stability of fragment 255−316 by 2.2 °C in terms of T_m, corresponding to an increase in the unfolding free energy change of 0.71 kcal/mol of monomer (Table 1). We show here that this stabilizing effect can be explained on the basis of a reduction of the backbone conformational entropy of unfolding.

For a given residue X, an approximate estimate of the unfolding entropy change can be obtained by the equation $\Delta S_{conf}(X) = R \ln(\gamma_U/\gamma_N)$, where γ_U and γ_N are the number of conformations available to residue X in the unfolded and native state, respectively (*61*). Considering that the 3D structure of the folded fragment 255−316 is not changed upon Ala → Aib replacement (see Results), then γ_N for Ala is very close to γ_N for Aib. Thus, it is possible to calculate the unfolding entropy change of Aib with respect to Ala as $\Delta S_{Ala\rightarrow Aib} = \Delta S_{conf}(Aib) - \Delta S_{conf}(Ala) = R \ln(\gamma_{Aib}/\gamma_{Ala})$, where γ_{Aib} and γ_{Ala} are the relative conformational space available to Aib and Ala, respectively. The replacement of the proton on the C_α atom of the Ala residue with a -CH_3 group greatly restricts the possible rotations about the N−C_α and C_α−C′ bonds. Indeed, the region of conformational space allowed to Ala ($\gamma_{Ala} = 38\%$) (*62*) is considerably reduced for Aib ($\gamma_{Aib} = 12\%$) (*31*). On this basis, the estimated backbone contribution to the entropy of unfolding of Aib relative to Ala is −2.2 cal/(deg·mol), which allows us to estimate a figure of ∼0.74 kcal/mol for the free energy change of unfolding, at $T_{m,wt}$, utilizing the equation $\Delta\Delta G_{conf} = -T_{m,wt}\Delta S_{Ala\rightarrow Aib}$, in excellent agreement with the difference in stability determined experimentally for the two fragment species (see Table 1).

The stabilizing effect of the Ala → Aib exchange in position 304 of fragment 255−316 is in line with that obtained by replacing Ala82 for Aib in T4-lysozyme, which is the single attempt at introducing Aib into proteins reported so far (*10*). However, the Ala82Aib mutant of T4-lysozyme was only ∼1 °C more stable than the wild-type protein. The lower stabilizing effect observed for T4-lysozyme compared to those observed here might be explained by considering that Ala82 is located at a short and flexible loop connecting two helices in T4-lysozyme and not at a segment of regular secondary structure, as Ala304 in the thermolysin fragment. In this respect, rigidification of a flexible site in a protein structure is expected to decrease the entropy of both unfolded and native states, thus resulting in a lower stabilizing effect (see also below). This view is in keeping with the results of a number of mutagenesis studies showing that loop regions tolerate extensive changes in amino acid composition with only small changes in protein stability (*63*) and suggesting that the effects of potentially stabilizing mutations in proteins are expected to be more pronounced when amino acid replacements are made at the level of the more rigid secondary structure elements (*64*).

Ala309Aib. The comparative analysis of the thermodynamic data reported in Table 1 shows that the replacement of Ala for Aib in position 309 stabilizes the protein domain more efficiently than in position 304. As discussed above for Ala304, the backbone geometry of Ala309 is compatible with the conformational restraints imposed by the Ala → Aib exchange (see Table 2). However, at variance from Ala304, which is a surface residue, Ala309 is completely buried in a hydrophobic environment (*39*), but allowing enough space for the two methyl groups of Aib to be placed inside the apolar interior of the protein domain, as verified by model building. Moreover, accessible surface area (ASA) calculations indicate that Aib309 is completely shielded from the aqueous solvent (see Table 2). Based on these considerations, it is proposed that the greater stabilizing effect observed for Ala → Aib exchange in position 309 with respect to that at position 304 can be approximated by the relationship $\Delta\Delta G_U = \Delta\Delta G_{conf} + \Delta\Delta G_\phi$, where the energy term $\Delta\Delta G_{conf}$ is the contribution to $\Delta\Delta G_U$ that arises from the reduction of the backbone conformational entropy (expected to be very close to that estimated for the Ala → Aib exchange in position 304, 0.74 kcal/mol), and $\Delta\Delta G_\phi$ represents the contribution of hydrophobic stabilization to the overall stability of protein domain 255−316.

It is widely accepted that the contribution of a given mutation to the hydrophobic stabilization of a protein can be estimated from the changes in the apolar surface area buried upon folding by the wild-type and mutant protein ($\Delta\Delta A_\phi$), multiplied for a proportionality constant. Based on theoretical (*65*) and experimental grounds (*66*), the value of this constant is taken as 20−25 cal/mol *per* Å^2 of apolar surface area buried. As given by the ASA values reported in Table 2, Aib309 buries more hydrophobic surface than Ala309 ($\Delta\Delta A_\phi$ = ∼45 Å^2), leading to an increase in ΔG_ϕ of ∼0.9−1.1 kcal/mol. This value of $\Delta\Delta G_\phi$ is that expected from the difference between the change in stability of the analog Ala309Aib determined experimentally ($\Delta\Delta G_U$ = 1.76 kcal/mol) and the contribution of the unfolding entropy change estimated from the Ala → Aib exchange in position 304 ($\Delta\Delta G_{conf}$ = 0.71 kcal/mol). It is of interest to note that a hydrophobic stabilization of ∼1 kcal/mol compares favorably with the gain in ΔG_U, estimated from protein engineering experiments, deriving from the addition of a -CH_3 group to a hydrophobic cavity in the absence of strain (1.0−1.4 kcal/mol) (*67*).

Ala312Aib. The Ala → Aib exchange in position 312 of fragment 255−316 slightly destabilizes the folded conformation of the fragment by ∼0.6 °C, which corresponds to a decrease in the free energy of unfolding of ∼0.2 kcal *per* mole of monomer (see Table 1). Ala312 is partially shielded from the solvent and, at variance from Ala304 or Ala309, is not embedded in the C-terminal helix 301−311. The backbone dihedral angles of Ala312 (see Table 2) are outside those allowed for the Aib residue (see above). Moreover, model building indicates that the presence of the extra -CH_3 of Aib312 tends to introduce prohibitively close contacts with the main-chain atoms of Asp311 and Val315. Notwithstanding, the overall 3D structure of fragment 255−316 is not changed upon Ala → Aib substitution (see Results), suggesting that Aib312 is forced by the global fold of the protein to acquire an unfavorable conformation. These findings are in line with the notion that protein structures can accommodate a larger side chain with little structural perturbations (*68*−*70*) and that, in general, the mutated residue adapts to the 3D environment in which it is embedded rather than the environment to the mutation (*71*, *72*). However, residues with ϕ, ψ angles outside their preferred conformation represent sites of local strain and have been found to destabilize the folded state of proteins by 0.5−2 kcal/mol (*73*−*75*). Hence, the lower stability of the analog Ala312Aib can be reasonably explained by considering that the potentially stabilizing effect of Ala → Aib exchange by the entropic effect (see above) is largely offset by unfavorable strain energy effects that destabilize the folded state of fragment 255−316. Moreover, simple entropic considerations allow us to propose that the Ala → Aib exchange at position 312 is expected to produce a lower stabilizing effect with respect to those at position 304 or 309, since Ala312 is a rather flexible residue, as given by the high value of the root mean square deviations of dihedral angles ϕ, ψ (see Table 2), and is located at the fraying C-terminal end of the protein domain 255−316 (*39*). The Ala → Aib exchange restricts the peptide backbone into a limited set of possible conformations, decreasing the entropy of the native state and leading to a smaller reduction of the unfolding entropy change (ΔS_{conf}) and correspondingly to a lower stabilizing effect of the Ala → Aib replacement.

Ala304Aib/Ala309Aib. A key result of the present study is that the stabilizing effect of Ala → Aib replacement at positions 304 and 309 is additive, if compared to the singly substituted Aib analogs (see Table 2). Additivity of mutational effects is often observed in proteins when mutations are relatively distant in the three-dimensional protein structure (*76*), as for example in subtilisin BPN′ (*77*), T4-lysozyme (*78*), *Bacillus subtilis* neutral protease (*35*), and gene V protein (*79*). Conversely, deviations from additive behavior can occur when the sites of mutation interact directly with each other (*80*, *81*) or indirectly through large structural perturbations (*82*−*84*), or when multiple amino acid replacements affect the properties of the denatured state to a different extent with respect to the single mutations (*85*). On this basis, the additivity of the stabilizing effects of Ala

→ Aib exchange in positions 304 and 309 can be taken as evidence that the sites of mutation behave independently, in the sense that the substitution of Ala304 for Aib does not affect the contribution to protein stability of the Ala → Aib replacement at position 309. Moreover, the observed additivity of mutational effects can be taken as an indication that the structural perturbations introduced by the amino acid replacements are restricted to the local environment of the mutation sites, as indeed inferred from CD spectroscopy (see Figure 3 and above).

Conclusions. Our results show that the rational incorporation into a globular protein of the conformationally constrained amino acid Aib can lead to significant stabilization of the protein structure. Considering also the results of previous studies conducted on Aib-containing peptides (*3*), it can be proposed that Aib exchange in a polypeptide chain has great potential for engineering protein stability, if a suitable procedure for the incorporation of Aib into a protein is found. Clearly, the results of this study indicate that semisynthesis can solve this problem, but a drawback of this procedure is that it requires significant experimental efforts in tailoring the technique to the specific protein system (availability of a suitable fragment system, choice of the protease and of the solvent conditions for the fragment ligation) (*18*, *20*). Nevertheless, once this problem has been overcome, the semisynthetic approach can be used to tackle protein engineering experiments that would be difficult or even impossible by using genetic methods (*86*). In this study, the Aib replacement was confined to Ala residue(s) located in the C-terminal helix of fragment 255−316. Since Ala is the most helix-forming amino acid among the 20 protein amino acids (*28*), it could well be that after performing Aib exchange(s) at other residues in helical segments in a protein, even more dramatic enhancements of protein thermal stability than those observed in the present study could be achieved.

ACKNOWLEDGMENT

We thank Claudio Toniolo for helpful advice and useful discussions and Francesco Tinazzi for having conducted some experiments reported in this study.

REFERENCES

1. Fersht, A. R., and Serrano, L. (1993) *Curr. Opin. Struct. Biol. 3*, 75−83.
2. Matthews, B. W. (1995) *Adv. Protein Chem. 46*, 249−278.
3. Balaram, P. (1992) *Curr. Opin. Struct. Biol. 2*, 845−851.
4. Benner, S. A. (1994) *TibTech 12*, 158−162.
5. Ibba, M., and Hennecke, H. (1994) *Biotechnology 12*, 678−682.
6. Mendel, D., Cornish, V. W., and Schultz, P. G. (1995) *Annu. Rev. Biomol. Struct. 24*, 435−462.
7. Beiboer, S. H., van den Berg, B., Dekker, N., Cox, R. C., and Verheijh, M. (1996) *Protein Eng. 9*, 345−352.
8. Wong, C.-Y., and Eftink, M. R. (1997) *Protein Sci. 6*, 689−697.
9. Noren, C. J., Anthony-Cahill, S. J., Griffith, M. C., and Schultz, P. G. (1989) *Science 244*, 182−188.
10. Ellman, J. A., Mendel, D., and Schultz, P. G. (1992) *Science 255*, 197−200.
11. Mendel, D., Ellman, J. A., Chang, Z., Veenstra, D. L., Kollman, P. A., and Schultz, P. G. (1992) *Science 256*, 1798−1802.
12. Chung, H.-H., Benson, D. R., and Schultz, P. G. (1993) *Science 259*, 806−809.
13. Cornish, V. W., Kaplan, M. I., Veenstra, D. L., Kollman, P. A., and Schultz, P. G. (1994) *Biochemistry 33*, 12022−12031.
14. Cornish, V. W., Benson, D. R., Altenbach, C. A., Hideg, K., Hubbell, W. L., and Schultz, P. G. (1994) *Proc. Natl. Acad. Sci. U.S.A. 91*, 2910−2914.
15. Mendel, D., Ellman, J. A., and Schultz, P. G. (1993) *Proc. Natl. Acad. Sci. U.S.A. 115*, 4359−4360.
16. Hohsaka, T., Sato, K., Sisido, M., Takai, K., and Yokoyama, S. (1993) *FEBS Lett. 335*, 47−50.
17. Kent, S. B. H. (1988) *Annu. Rev. Biochem. 57*, 957−989.
18. Chaiken, I. M. (1981) *CRC Crit. Rev. Biochem. 11*, 255−301.
19. Wallace, C. J. A., Guillemette, J. G., Hibiya, Y., and Smith, M. (1991) *J. Biol. Chem. 266*, 21355−21357.
20. Wallace, C. J. A. (1995) *Curr. Opin. Biotechnol. 6*, 403−410.
21. Homandberg, G. A., and Laskowski, M., Jr. (1979) *Biochemistry 18*, 586−592.
22. Nagaraj, R., and Balaram, P. (1981) *Acc. Chem. Res. 14*, 356−363.
23. Karle, I. L., and Balaram, P. (1990) *Biochemistry 29*, 6747−6756.
24. Toniolo, C., and Benedetti, E. (1991) *Macromolecules 24*, 4004−4009.
25. Pavone, V., Benedetti, E., Di Blasio, B., Pedone, C., Santini, A., Bavoso, A., Toniolo, C., and Crisma, M. (1990) *J. Mol. Biol. 214*, 633−635.
26. Toniolo, C., and Benedetti, E. (1991) *Trends Biochem. Sci. 16*, 350−353.
27. Marshall, G. R., Hodgkin, E. E., Langs, D. A., Smith, G. D., Zabrocki, J., and Leplawy, M. T. (1994) *Proc. Natl. Acad. Sci. U.S.A. 87*, 487−491.
28. O'Neil, K. T., and DeGrado, W. F. (1990) *Science 250*, 646−651.
29. Hermans, J., Anderson, A. G., and Yun, R. H. (1992) *Biochemistry 31*, 5646−5653.
30. Burgess, A. W., and Leach, S. (1973) *Biopolymers 12*, 2599−2605.
31. Paterson, Y., Rumsey, S. M., Benedetti, E., Némethy, G., and Scheraga, H. A. (1981) *J. Am. Chem. Soc. 103*, 2947−2955.
32. Burgess, A. W. (1994) *Proc. Natl. Acad. Sci. U.S.A. 91*, 2649−2653.
33. Matthews, B. W., Nicholson, H., and Becktel, W. J. (1987) *Proc. Natl. Acad. Sci. U.S.A. 84*, 6663−6667.
34. Takagi, M., and Imanaka, T. (1989) *FEBS Lett. 254*, 43−46.
35. Margarit, I., Campagnoli, S., Frigerio, F., Grandi, G., De Filippis, V., and Fontana, A. (1992) *Protein Eng. 5*, 543−550.
36. Augspurger, J. D., Bindra, V. A., Scheraga, H. A., and Kuki, A. (1995) *Biochemistry 34*, 2566−2576.
37. Holmes, M. A., and Matthews, B. W. (1982) *J. Mol. Biol. 160*, 623−639.
38. Dalzoppo, D., Vita, C., and Fontana, A. (1985) *J. Mol. Biol. 182*, 331−340.
39. Rico, M., Jiménez, M. A., Gonzáles, C., De Filippis, V., and Fontana, A. (1994) *Biochemistry 33*, 14834−14847.
40. Conejero-Lara, F., De Filippis, V., Fontana, A., and Mateo, P. (1994) *FEBS Lett. 344*, 154−156.
41. De Filippis, V., and Fontana, A. (1990) *Int. J. Pept. Protein Res. 35*, 219−227.
42. Fassina, G., Vita, C., Dalzoppo, D., Zamai, M., Zambonin, M., and Fontana, A. (1986) *Eur. J. Biochem. 156*, 221−228.
43. Drapeau, G. R. (1977) *Methods Enzymol. 47*, 189−191.
44. Atherton, E., and Sheppard, R. C. (1987) in *The Peptides* (Udenfriend, S., and Meienhofer, J., Eds.) Vol. 9, pp 1−39, Academic Press, New York.
45. Wang, S. S. (1973) *J. Am. Chem. Soc. 95*, 1328−1333.
46. Knorr, R., Trzeciak, A., Bannwarth, W., and Gillessen, D. (1989) *Tetrahedron Lett. 30*, 1927−1930.
47. Milton, R. C., Milton, S. C. F., and Adams, P. A. (1990) *J. Am. Chem. Soc. 112*, 6039−6046.
48. Heinrikson, R. L., and Meredith, S. C. (1984) *Anal. Biochem. 136*, 65−74.

49. Gill, S. G., and von Hippel, P. H. (1989) *Anal. Biochem. 182*, 319−326.
50. Toumadje, A., Alcorn, S. W., and Johnson, W. C., Jr. (1992) *Anal. Biochem. 200*, 321−331.
51. Becktel, W. J., and Schellman, J. A. (1987) *Biopolymers 26*, 1859−1877.
52. Privalov, P. L. (1979) *Adv. Protein Chem. 33*, 167−241.
53. Richards, F. R. (1985) *Methods Enzymol. 115*, 440−464.
54. Conejero-Lara, F., and Mateo, P. L. (1996) *Biochemistry 35*, 3477−3486.
55. Slomczynska, U., Beusen, D. D., Zabrocki, J., Kociolek, K., Redlinski, A., Reusser, F., Hutton, W. C., Leplawy, M. T., and Marshall, G. R. (1992) *J. Am. Chem. Soc. 114*, 4095−4097.
56. Sapia, A. C., Slomczynska, U., and Marshall, G. R. (1994) *Lett. Pept. Sci. 1*, 283−290.
57. Brahms, S., and Brahms, J. (1980) *J. Mol. Biol. 138*, 149−178.
58. Strickland, E. H. (1974) *CRC Crit. Rev. Biochem. 3*, 113−175.
59. Woody, R. W. (1995) *Methods Enzymol. 246*, 34−71.
60. Loll, P. J., and Lattman, E. E. (1990) *Biochemistry 29*, 6866−6873.
61. Némethy, G., Leach, S. J., and Scheraga, H. A. (1966) *J. Phys. Chem. 70*, 998−1004.
62. Zimmerman, S. S., Pottle, M. S., Némethy, G., and Scheraga, H. A. (1977) *Macromolecules 10*, 1−9.
63. Brunet, A. P., Huang, E. S., Huffine, M. E., Loeb, J. E., Weltman, R. J., and Hecht, M. H. (1993) *Nature 364*, 355−358.
64. Alber, T., Dao-Pin, S., Nye, J. A., Muchmore, D. C., and Matthews, B. W. (1987) *Biochemistry 26*, 3754−3758.
65. Chothia, C. (1974) *Nature 248*, 338−339.
66. Eriksson, A. E., Baase, W. A., Zhang, X.-J., Heinz, D. W., Blaber, M., Baldwin, E. P., and Matthews, B. W. (1992) *Science 255*, 178−183.
67. Eriksson, A. E., Baase, W. A., and Matthews, B. W. (1993) *J. Mol. Biol. 229*, 747−769.
68. Hurley, J. H., Baase, W. A., and Matthews, B. W. (1992) *J. Mol. Biol. 224*, 1143−1159.
69. Lim, W. A., Farruggio, D. C., and Sauer, R. T. (1992) *Biochemistry 31*, 4324−4333.
70. Buckle, A. M., Henrick, K., and Fersht, A. R. (1993) *J. Mol. Biol. 234*, 847−860.
71. De Filippis, V., Vriend, G., and Sander, C. (1994) *Protein Eng. 7*, 1203−1208.
72. Laughton, C. A. (1994) *J. Mol. Biol. 235*, 1088−1097.
73. Nicholson, H., Soderlind, E., Tronrud, D. E., and Matthews, B. W. (1989) *J. Mol. Biol. 210*, 181−193.
74. Dao-Pin, S., Baase, W. A., and Matthews, B. W. (1990) *Proteins: Struct., Funct., Genet. 7*, 198−204.
75. Stites, W. E., Meeker, A. K., and Shortle, D. (1994) *J. Mol. Biol. 235*, 27−32.
76. Wells, J. A. (1990) *Biochemistry 29*, 8509−8517.
77. Pantoliano, M. W., Whitlow, M., Wood, J. F., Dodd, S. W., Hardman, K. D., Rollence, M. L., and Bryan, P. N. (1989) *Biochemistry 28*, 7205−7213.
78. Zhang, X.-J., Baase, W. A., Shoichet, B. K., Wilson, K. P., and Matthews, B. W. (1995) *Protein Eng. 8*, 1017−1022.
79. Sandberg, W. S., and Terwillinger, T. C. (1993) *Proc. Natl. Acad. Sci. U.S.A. 90*, 8367−8371.
80. Dao-Pin, S., Alber, T., Baase, W. A., Wozniak, J. A., and Matthews, B. W. (1991) *J. Mol. Biol. 221*, 647−667.
81. Mildvan, A. S., Weber, D. J., and Kuliopulos, A. (1992) *Arch. Biochem. Biophys. 294*, 327−340.
82. Shortle, D., and Meeker, A. K. (1986) *Proteins: Struct., Funct., Genet. 1*, 81−89.
83. Robinson, C. R., and Sligar, S. G. (1993) *Protein Sci. 2*, 826−834.
84. LiCata, V. J., and Ackers, G. K. (1995) *Biochemistry 34*, 3133−3139.
85. Green, S. M., and Shortle, D. (1993) *Biochemistry 32*, 10131−10139.
86. Offord, R. E. (1987) *Protein Eng. 1*, 351−357.
87. Miller, S., Janin, J., Lesk, A. M., and Chothia, C. (1987) *J. Mol. Biol. 196*, 641−656.
88. Kraulis, P. J. (1991) *J. Appl. Crystallogr. 24*, 946−950.
89. Titani, K., Hermodson, M. A., Ericsson, L. H., Walsh, K. A., and Neurath, H. (1972) *Biochemistry 11*, 2427−2435.

BI971937O